

Chiral Discrimination Effects in Langmuir Monolayers: Monolayers of Palmitoyl Aspartic Acid, *N*-Stearoyl Serine Methyl Ester, and *N*-Tetradecyl- γ,δ -dihydroxypentanoic Acid Amide

N. Nandi[†] and D. Vollhardt^{*‡}

Chemistry Department, Birla Institute of Technology and Science, Pilani, Rajasthan, 333031, India, and
Max Planck Institute of Colloids and Interfaces, D-14424, Potsdam/Golm, Germany

Received: August 9, 2002; In Final Form: December 10, 2002

The chiral discrimination energies in domains composed of chiral amphiphilic monolayers are theoretically studied. First, calculations on simpler model systems are carried out which show that the depth of the pair potential well is dependent on the extent of coarse-graining the molecular structure. However, systematic coarse-graining of model systems shows that the consistent use of a set of parameters can correctly predict the chiral preference (homo- or heterochirality). The model calculation further suggests that, with a gradual loss of chirality of the model molecule, the chiral interaction is diminished. Calculations of the chiral discriminating pair potential of three chiral compounds, *N*-stearoyl serine methyl ester, *N*-palmitoyl aspartic acid, and *N*-tetradecyl- γ,δ -dihydroxypentanoic acid amide indicate homochiral preference. The preference is observed both in packing of a pair of molecules and the pair potential energy profile. The enantiomeric pairs are closely packed and have a lower minimum pair potential compared to the racemic pairs. The homochiral preference corroborates well with the domain features observed by BAM. The growth in both directions observed in racemic domains are suggestive of local chiral symmetry breaking, which is possible in the case of the homochirally preferred interaction. We also compare the results of the calculation of discrimination energy by the present approach and the results by other molecular models available in the literature. Whereas the basic conclusions of the present model and other models agree, the present model reveals a nontrivial distance and orientation dependence of the discrimination energy. The results are insensitive to the choice of parameters.

Introduction

The calculation of the chiral interaction energy is of continued interest^{1–17} due to the omnipresence of chiral interactions in biological and biomimetic systems.^{18–20} Chirality is present in many biological systems at microscopic, mesoscopic and macroscopic levels. Common examples are proteins and their constituent amino acids, nucleic acids, and their constituent sugars as well as membranes and their constituent lipids and membrane proteins. Surprisingly, in the most cases, only one enantiomer of the basic building blocks of life is biologically active. Why Nature prefers only one enantiomer remained a puzzle. The small energy difference between the two enantiomeric forms poses a further challenge to understand the famous *problem of homochiral evolution*.¹⁹

Chirality effects are well-known in monolayers.^{1,7–17} Chiral discrimination is apparent in differences in the morphology or the physical behavior of a monolayer system as a function of its enantiomeric content. It is expected that the discrimination effect will be observed in the condensed phase where the chiral interactions become significant. The discriminating behavior can be concluded from different experimental techniques, such as π -A isotherm measurements and from optical techniques, such as Brewster angle microscopy (BAM); as well as from lattice

structural information based on grazing incidence X-ray diffraction (GIXD) studies. The discrimination is manifested in various ways, such as the shape and characteristic features of the isotherm, the shapes of the domains formed in the condensed phase, or differences in the lattice structures of the enantiomeric (or its mirror image) and racemic mixtures.

Different chiral features of domains composed of enantiomeric and racemic amphiphiles of *N*-tetradecyl- γ,δ -dihydroxypentanoic acid amide (TDHPAA), *N*-stearoyl serine methyl ester (SSME), and *N*-palmitoyl aspartic acid monolayers (PAA) are shown in Figures 1–3. The discriminating features are clear from the differences in the structural features of the domains composed of *D*-, *L*-, and *DL* (racemic) amphiphiles. The bifurcation of a small arm from *S*-enantiomer of TDHPAA develops in an exactly opposite direction to the development of the bifurcation of a similar smaller arm from *R*-enantiomer (Figure 1). The racemate seems to grow rather symmetrically from a common center. It is possible that a defect develops with specific orientation in the enantiomeric monolayer and the smaller arm develops in enantiomeric TDHPAA. In racemates, the chiral symmetry breaking takes place with enantiomeric excess by the two sides of a common center. In SSME and PAA (Figures 2 and 3), the directions of curvature of the enantiomeric domains are of specific handedness and the racemates show the development of both forms of handedness. The development of arms of both handedness from the racemate could possibly be a signature of chiral symmetry breaking in SSME monolayers.

* Corresponding author. (N. Nandi) E-mail: nnandi@bits-pilani.ac.in. FAX: 91-159-76-44183. (D. Vollhardt) E-mail: vollh@mpikg-golm.mpg.de. FAX: 49-331-567-9202.

[†] Chemistry Department.

[‡] Max Planck Institute of Colloids and Interfaces.

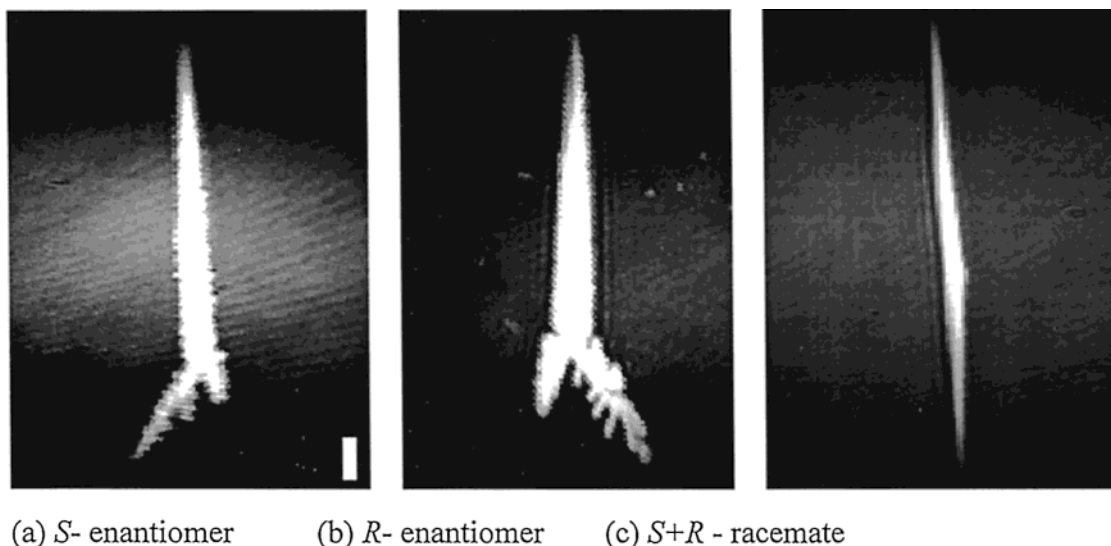


Figure 1. Chiral discrimination of the condensed phase textures of *N*-tetradecyl- γ,δ -dihydroxy-pentanoic acid amide monolayers.

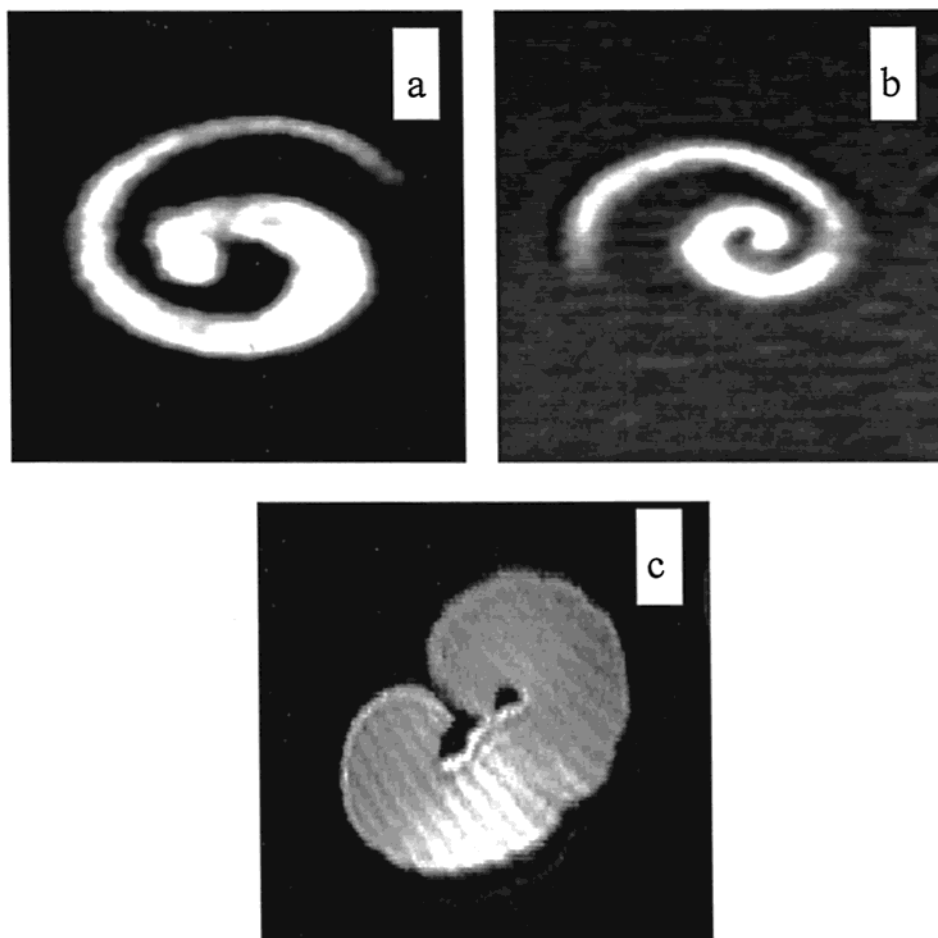


Figure 2. Chiral discrimination of the condensed phase domains of *N*-stearoyl serine methyl ester monolayers spread on pH 3 water. (a) *D*-enantiomer (b) *L*-enantiomer (c) and (d) 1:1 *DL* racemate. Image size $80 \times 80 \mu\text{m}$.

A complete understanding of the underlying mechanism of the discriminating effect is yet to be developed. From the viewpoint of the interaction at the molecular level, two types of interactions can take place. If *D*–*D* or *L*–*L* interaction is favored over the *D*–*L* interaction, it is called “homochiral interaction”. On the other hand, if the interaction of the two different enantiomers (*D*–*L*) is more favored compared to the interaction between a pair of the same type of enantiomers (*D*–*D* or *L*–*L*), it is called “heterochiral interaction”. If the

homochiral interaction is sufficiently strong, then it is possible that *D*-rich or *L*-rich domains would separate out from a racemic mixture. Such phase separation is an example of “chiral symmetry breaking”. As indicated previously, chiral symmetry breaking is related to the origin of the homochiral evolution. However, in many cases the conclusions about the preferred chiral interaction (homo- or hetero-) from experimental studies using different techniques are at variance. Furthermore, the measurements of π -*A* isotherm, BAM, and GIXD often show

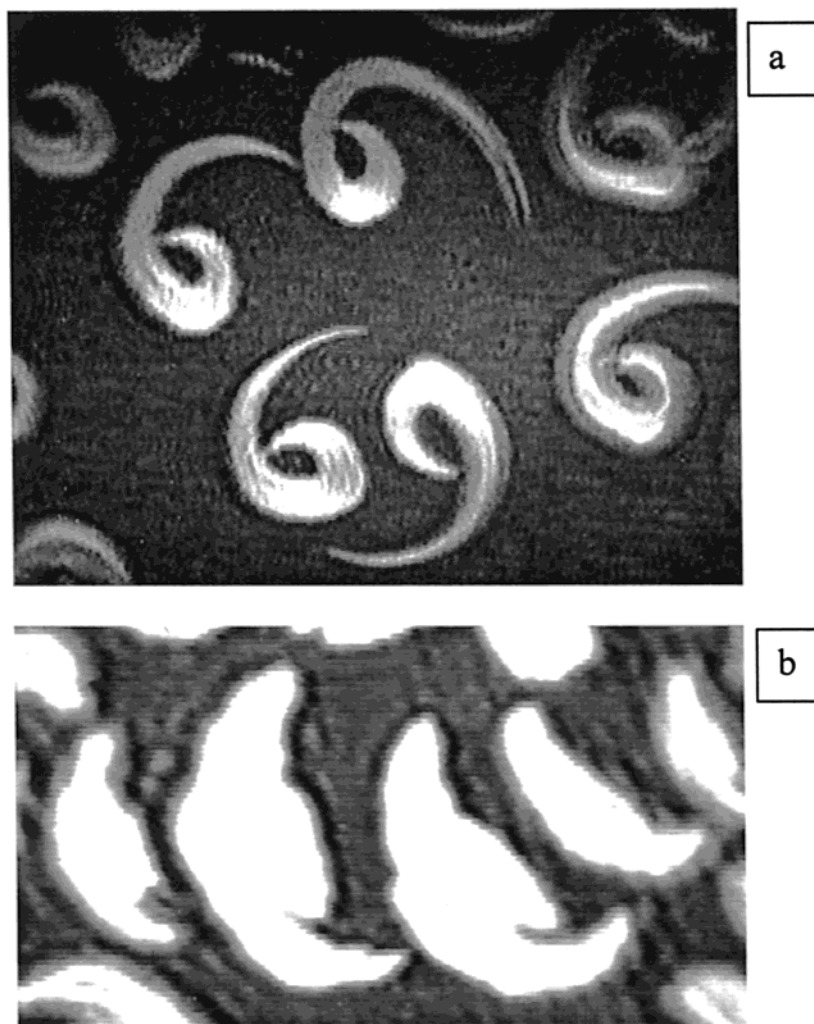


Figure 3. Chiral discrimination of the condensed phase domains of *N*-palmitoyl aspartic acid monolayers spread on pH 3 water. (a) *D*-enantiomer, image size $400 \times 320 \mu\text{m}$. (b) 1:1 *DL* racemate, image size $100 \times 50 \mu\text{m}$.

different sensitivity to the chiral preferences. The isotherm studies measure thermodynamic quantities, which are macroscopic properties such as surface pressure. On the other hand, GIXD probes the lattice dimensions in the range of molecular length scale characteristic of the monolayer system. The underlying interactions have different relative weightiness in two experiments because of the different ranges of the interactions. Thus, it is not surprising that two different methods predict different chiral sensitivities.

Only in recent years, the direct observation of chiral segregation in monolayers has been made on the basis of optical methods (BAM) and GIXD studies. Early conclusions on chiral segregation based only on the behavior of π -*A* isotherm of racemates should be judged with caution as numerous other phenomena can affect the surface tension. It is important to note that *both* hetero- and homochirality are observed experimentally, and it is still unclear which interaction is dominant in which amphiphilic system.

Different theoretical approaches are taken in calculating the chiral interaction. Two broad classes of theories are continuum and molecular theories. In the continuum approach, the microscopic features of the system present at the molecular length scale are neglected. It is obvious that it is not possible to have a quantitative estimation of the interaction energy of chiral molecules from such a calculation. Being less abstract, molecular theories are promising to calculate chiral interaction energies in biomimetic systems. Different molecular approaches are

available. The origin of chiral shapes in monolayers is discussed in the literature.^{1,12,13} Andelman and De Gennes²⁻⁴ developed an important molecular model for chiral interaction. In recent years, another theory has been developed, which considers the *effective pair potential* (EPP) between the chiral molecules.⁶⁻¹¹ The EPP is calculated from the consideration of the detailed molecular chiral structure. It is pointed out that the subtle stereogenicity at the chiral center of a molecule is the driving force for the chiral features (like specific curvature or handedness) in the shape of the aggregate composed of the molecules.

It is worthwhile to investigate the chiral discrimination energy using molecular approaches. Andelman and co-workers carried out the most important theoretical work in this direction. The difference between the second virial coefficient of the pure enantiomeric monolayer and the same of the racemic monolayer is proposed as a chiral discrimination parameter.⁴ The calculation based on Boltzmann-weighted averaging of molecular interactions predicts a preferred heterochiral behavior for van der Waals interactions and homochiral behavior for electrostatic interactions. It might be noted that hydrogen-bonding interactions (which are of primarily electrostatic origin) are dominant in several amphiphilic monolayers (for example, amphiphiles containing amino acid or amide headgroups). Consequently, a competition between the homochiral (which could originate from van der Waals interaction) and heterochiral interaction (which could originate from hydrogen bonding or other electrostatic interactions, such as those between the partial charges on the

segments of headgroups) might take place in these monolayers. In these cases, the chiral preference is still far from understood.

Monte Carlo simulation was also carried out to study the chiral discrimination of *D*- and *L*-alanine. Homochiral preference was observed which is suggested to arise from the short-range steric interactions. However, calculation of the chiral discrimination energy using an atomistic description of large molecules is computationally extensive. To reduce the difficulty of the calculation, rigid-tetrahedral-shaped molecules are also considered as molecular model. The rigidity in shape reduces the number of degrees of freedom to five.⁴ In this model, heterochiral preference is observed for the Lennard-Jones (LJ) potential. It is also observed that the chiral preference is dependent on the intermolecular separation. At short separations homochirality is favored whereas at larger distances heterochirality is favored.

In the present paper we first compare the results of coarse-grained (CG) and equivalent sphere (ES) approaches for model systems in section 2.B. The objective is to investigate the effect of coarse-graining on the conclusion of chiral discrimination energy. Then we calculate the discrimination energy for SSME, PAA, and TDHPAA.

Theoretical Calculation

The intermolecular interaction energy between the groups composing tails and heads of the two molecules is given by a Lennard-Jones potential and represents the short-range repulsion and long-range attraction over all nonbonded pairs of groups (*g*) of the *i*th and *j*th molecules.

$$U/k_B T = \sum_{\substack{g(i) \\ g(j)}} (4/T) (\epsilon^{g(i)g(j)}/k_B) [(s^{g(i)g(j)}/\sigma^{g(i)g(j)})^{-12} - (s^{g(i)g(j)}/\sigma^{g(i)g(j)})^{-6}] \quad (1)$$

Here, $s^{g(i)g(j)}$ is the orientation dependent distance between the $g(i)$ and $g(j)$ groups,^{9,10} $\sigma^{g(i)g(j)}$ is the average Lennard-Jones diameter of the corresponding groups, and the energy parameter $\epsilon^{g(i)g(j)}$ is given by the Berthelot rule:

$$\epsilon^{g(i)g(j)} = (\epsilon^{g(i)} \epsilon^{g(j)})^{1/2} \quad (2)$$

Comparison of the Equivalent Sphere (ES) and the Coarse-Grained (CG) Approach To Calculate the Chiral Interaction. In the equivalent sphere (ES) based approach, the molecule is considered to be composed of a minimum number of spherical groups attached to each chiral center present in the molecule. Each of these groups may be composed of one or more groups, such as CH₂, CH₃, CH, and COO groups, for example. The details at the atomistic or at the length scale of smaller group (like those mentioned previously) are neglected in the ES approach. However, the effective sphericalization of the groups should be such that not to destroy the chirality of the chiral center(s) present in the molecule. For example, a chiral amphiphilic molecule is composed of minimum four different groups attached to a common chiral carbon atom. It is not possible to reduce the number of groups any further (by combining groups into one or more larger equivalent sphere(s)) without losing the chirality. The effective diameters of the groups can be calculated from the group increment data tabulated by Bondi²² and using the empirical relations provided by Ben Amotz and Herschbach.²³ It is known that the energy parameter for alkanes is also linearly dependent on the size of the group.²² For 1 Å increase in the effective size of the group, ϵ/k_B increases by ~100 K.²³

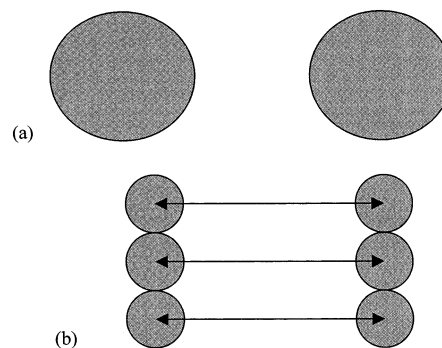


Figure 4. (a) A pair of LJ centers according to equivalent sphere representation. The pairs are shown in (b) after coarse-graining into 3 LJ centers. The arrows indicate the distances between the interacting centers.

In the coarse-grained (CG) approach, the tails and the heads of the molecule are represented by an array of collinear spherical groups (CH₂, CH₃, CH, COO groups etc.). For example, an alkyl chain like the palmitoyl chain can be considered as composed by one CH₃ group, fifteen CH₂ groups and one COO group. Thus, if one breaks the equivalent spheres attached to the chiral center present in the ES description (obeying the spatial molecular arrangement), it is possible to arrive at the molecular structure according to CG description. Thus, one grains the larger equivalent spheres into smaller basic units (spherical groups). These basic units need not be an atom but could be groups, such as CH₂, CH₃, CH, COO groups, etc. The atomistic detail of the molecular structure is neglected (one does not consider the individual carbon, hydrogen or oxygen atoms separately as interaction centers) but the CG description is certainly more detailed than the ES representation. The average orientations and distances of the groups with respect to the chiral center are considered accurately over a reasonably small length scale. These tails and heads are denoted by the subscripts “t” and “h”, respectively. A schematic diagram of the equivalent sphere description and coarse-graining of a molecular segment are shown in Figure 4. A similar representation applies to a whole molecule also. The natural question is whether the ES and CG representation give the same result for chiral interaction energy calculation. We first consider a simple calculation to address this question.

Equation 1 is a sum of the LJ potentials corresponding to the pairs of groups present in a pair of molecules. It is well-known that, for a single LJ pair, the depth of the pair potential well is $U_{\min} = -\epsilon$ and the separation at the minima is $2^{1/6}\sigma$. In the CG approach, the pair potential is the sum of more than one LJ potential term. In the simplest case, the potentials are only r dependent. In this special case, the orientation dependent distance, s is to be replaced by the separation between the groups, r . The following simple form gives the total pair potential

$$V/k_B T = \sum_{ij} (4/T) (\epsilon_{ij}/k_B) [(\sigma_{ij}/r)^{12} - (\sigma_{ij}/r)^6] \quad (3)$$

Here, r is the distance between each center (denoted by i, j) shown by the arrow in Figure 4. The minimum at the total pair potential is obtained at

$$r_{\min}(\text{CG}) = 2^{1/6} [(\sum_i \sigma_i^{12}) / (\sum_i \sigma_i^6)]^{1/6} \quad (4)$$

Thus, in the coarse-grained description of the molecule as shown in Figure 4b (here interaction centers are $i = 3$), one can

calculate the interactions by neglecting the diagonal interactions and considering only $i = j$ interactions (in this case, the distance between the interacting centers is always r). The location of the minima in the two approaches would be related as follows:

$$r_{\min}(\text{CG})/r_{\min}(\text{ES}) = \sigma_i(\text{CG})/\sigma(\text{ES}) \quad (5)$$

Here, all the groups have the same diameter. In the two cases, the depth of the potential would be related as follows

$$V(r_{\min}; \text{CG})/U(r_{\min}; \text{ES}) = [(\sum_i \epsilon_{\text{CG}} \sigma_{\text{CG}}^6)^2 / (\sum_i \epsilon_{\text{CG}} \sigma_{\text{CG}}^{12})] (1/\epsilon_{\text{ES}}) \quad (6)$$

The simple relation given by eq 6 shows that the depth of the potential is dependent on the extent of coarse-graining and may not be the same for the CG and ES approach.

Another important question is how this variance in the two approaches may affect the prediction of the chiral discrimination energy. To understand this, one needs to consider the orientation dependent pair potential (because one needs to take into account the orientation of the spatially distributed groups to consider the enantiomer and its mirror image). Suppose the azimuthal projection of the tail group is represented by α , the tilt by μ , and $\delta\alpha$ is the difference of the mutual azimuthal orientation of a pair (if any), then a set of exact geometric relations is developed from the tetrahedral geometry around the chiral center to express the orientation dependent distances s between the groups.^{9,10} Let us assume, for the tail–tail interaction, the functional of the orientation dependent distance is $f_{\text{tt}}(r, \alpha, \mu, \delta\alpha)$, for the head–head interaction it is $f_{\text{hh}}(r, \alpha, \mu, \delta\alpha)$, and for the remaining group (around the chiral center) it is $f_{\text{aa}}(r, \alpha, \mu, \delta\alpha)$. The interactions between tail–head, head–a group, and tail–a group are calculated by using the related distance functionals $f_{\text{th}}(r, \alpha, \mu, \delta\alpha)$, $f_{\text{ta}}(r, \alpha, \mu, \delta\alpha)$, and $f_{\text{ha}}(r, \alpha, \mu, \delta\alpha)$. In many cases, the fourth group is H and contributes negligibly to the pair potential. Also assume that there are i, j , and k number of the pairs of the tail, the head, and the remaining group existing for a pair of molecules. Then

$$\begin{aligned} V(r, \alpha, \mu, \delta\alpha)/k_{\text{B}}T = & \sum_{\text{tt}} (4/T)(\epsilon_{\text{tt}}/k_{\text{B}})[(\sigma_{\text{tt}}/f_{\text{tt}}(r, \alpha, \mu, \delta\alpha))^{12} - (\sigma_{\text{tt}}/f_{\text{tt}}(r, \alpha, \mu, \delta\alpha))^6] + \\ & \sum_{\text{hh}} (4/T)(\epsilon_{\text{hh}}/k_{\text{B}})[(\sigma_{\text{hh}}/f_{\text{hh}}(r, \alpha, \mu, \delta\alpha))^{12} - (\sigma_{\text{hh}}/f_{\text{hh}}(r, \alpha, \mu, \delta\alpha))^6] + \\ & \sum_{\text{aa}} (4/T)(\epsilon_{\text{aa}}/k_{\text{B}})[(\sigma_{\text{aa}}/f_{\text{aa}}(r, \alpha, \mu, \delta\alpha))^{12} - (\sigma_{\text{aa}}/f_{\text{aa}}(r, \alpha, \mu, \delta\alpha))^6] + \\ & \sum_{\text{th}} (4/T)(\epsilon_{\text{th}}/k_{\text{B}})[(\sigma_{\text{th}}/f_{\text{th}}(r, \alpha, \mu, \delta\alpha))^{12} - (\sigma_{\text{th}}/f_{\text{th}}(r, \alpha, \mu, \delta\alpha))^6] + \\ & \sum_{\text{ta}} (4/T)(\epsilon_{\text{ta}}/k_{\text{B}})[(\sigma_{\text{ta}}/f_{\text{ta}}(r, \alpha, \mu, \delta\alpha))^{12} - (\sigma_{\text{ta}}/f_{\text{ta}}(r, \alpha, \mu, \delta\alpha))^6] + \\ & \sum_{\text{ha}} (4/T)(\epsilon_{\text{ha}}/k_{\text{B}})[(\sigma_{\text{ha}}/f_{\text{ha}}(r, \alpha, \mu, \delta\alpha))^{12} - (\sigma_{\text{ha}}/f_{\text{ha}}(r, \alpha, \mu, \delta\alpha))^6] \end{aligned} \quad (7)$$

In most of the cases, the presence of several groups and the complicated functional forms for f_{tt} , f_{hh} , f_{aa} , f_{th} , f_{ta} , and f_{ha} prevent to obtain a straightforward analytical solution of eq 7. However, it is necessary to obtain the estimate how V_{\min} is affected by coarse-graining for the enantiomeric as well as racemic pair in order to obtain a clear understanding of the chiral discrimination. We study therefore model systems to understand how the

conclusion about the homo- and heterochirality is affected by the modeling scheme of the amphiphile.

Study of Model Systems. To understand the effect of coarse-graining on the results of the calculation of the chiral discrimination energy, we carried out numerical calculations using our previously developed relations^{9,10} for model systems as follows. The model system is shown schematically in Figure 5. The molecule is composed of two parts: one tail with a total volume that gives an equivalent sphere diameter of 8 Å and a head that gives an equivalent sphere diameter of 9 Å. The tilt of the tail group from the normal Z is taken as 25°. The orientation of the headgroup is determined by the fact that the tail and head have a mutual angle of 110° (the angle between two groups in a tetrahedral geometry around a chiral carbon). The azimuthal projections of the tail and headgroups are taken as 45° and 35°, respectively. The molecule is attached to the XY plane like an amphiphile at the interface. The restriction that the tail group cannot go below the XY plane or the headgroup cannot move above the XY plane together with the different azimuthal tilts of the tail and the headgroup, as used in the calculation, breaks the symmetry of the molecule. The molecule is coarse-grained gradually by breaking each tail and headgroups into 2, 3, and 5 pieces. This is shown in Figure 6. The diameters are reduced by the factors of $1/2$, $1/3$, and $1/5$, respectively. Note that the method of obtaining of the coarse-grained size is to be done according to the standard methods using the standard parameters given in the literature.^{22,23} Here, we do not concentrate on a specific molecule and obtain straightforwardly by taking representative examples. However, the range of coarse-grained diameter considered is sufficiently broad to cover a large number of chemical species (see parameters of several compounds provided in ref 23). The used parameters are shown in Table 1. We calculate the pair potential of the pair of enantiomers and a pair of mirror image isomers in each case. Mutual orientation is not allowed between the molecules. We minimize the energy and the obtained results are shown in Table 2.

Study of Amphiphilic Systems (N+–Stearoyl Serine Methyl Ester, Palmitoyl Aspartic Acid, and N-Tetradecyl- γ , δ -dihydroxypentanoic Acid Amide). We use the ES model of *N*-stearoyl serine methyl ester (abbreviated as SSME), palmitoyl aspartic acid (abbreviated as PAA), and *N*-tetradecyl- γ , δ -dihydroxypentanoic acid amide (abbreviated as TDHPAA) to study the chiral discrimination. The pair potential and handedness of the domains composed of the enantiomeric SSME and PAA have been studied before.¹⁰ In this study it is found that the ES model can predict the handedness of the domains correctly. Here, we calculate the pair potentials for the racemates of SSME and PAA and compare them with the features of the enantiomeric monolayers. We also calculate the pair potential for the enantiomeric and racemic TDHPAA. The parameters necessary for the computation are given in Table 3. For details of the parameters and expressions necessary for calculations, we refer to the literature previously published.¹⁰ In this calculation we allow the azimuthal projection of the second molecule to orient by 2π with respect to the first molecule. The variation in orientation allows probing the complete range of mutual orientation between the molecules. The results are described in the next section.

Results and Discussion

The results shown in Table 2 indicate that coarse-graining has influence on both the packing of molecules (indicated by the separation of the chiral centers at the minimum of the pair potential, r_{\min}) as well as the minimum of the pair potential

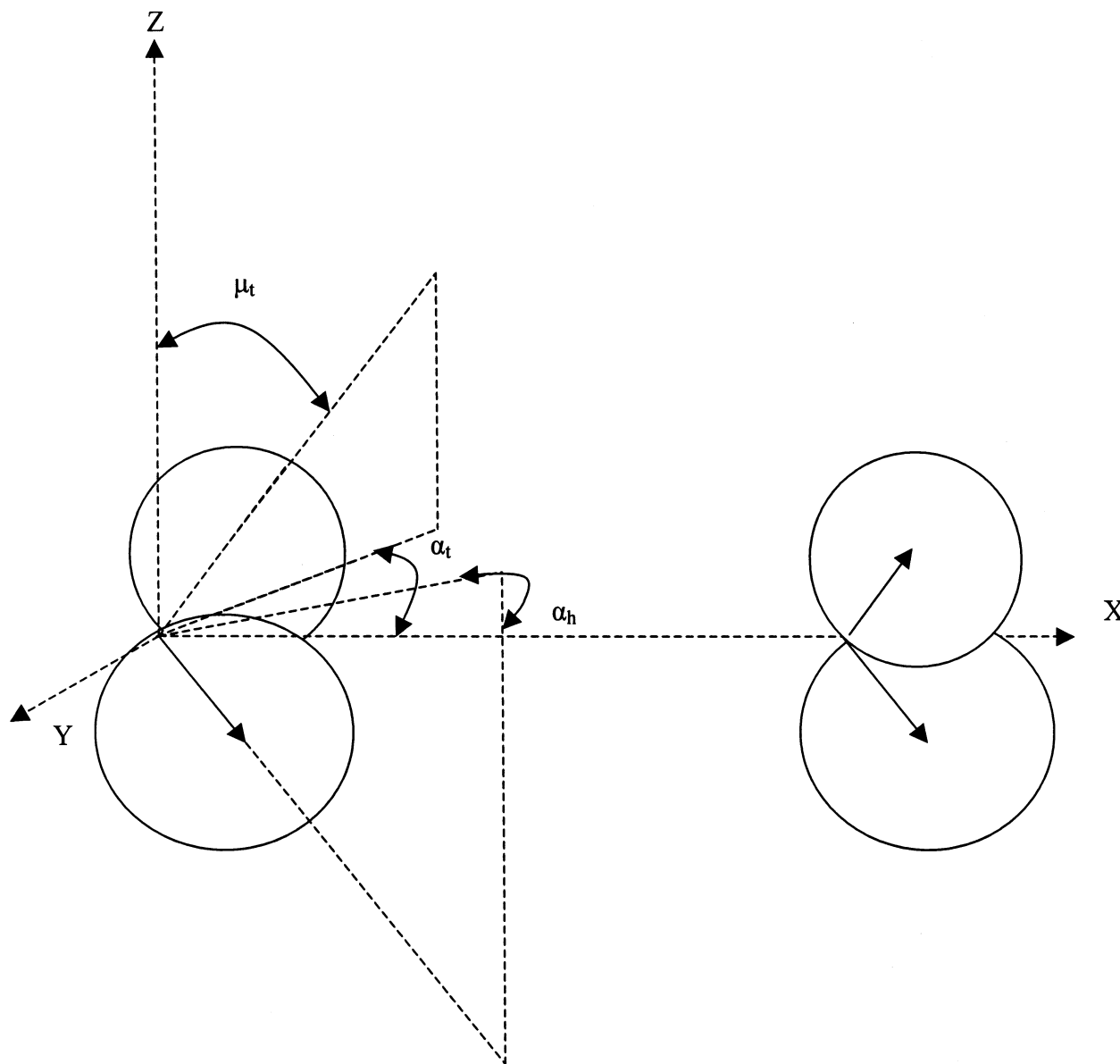


Figure 5. A pair of LJ centers and their spatial geometry according to the ES description.

($U_{\min}/k_B T$). The $U_{\min}/k_B T$ for the enantiomeric pairs becomes more stable with coarse-graining and the same for the racemic pair becomes less stable with coarse-graining. The $\Delta U_{\min}/k_B T$, which is the difference of the minimum pair potential of the enantiomers and racemates ($[U_{\min}(\text{En}) - U_{\min}(\text{Ra})]/k_B T$), becomes more negative as the molecule is more grained. The $\Delta U_{\min}/k_B T$ can be taken as a measure for the discrimination in the pair potential.

The observation can be explained by packing consideration. In Figures 4 and 5, the pairs of enantiomeric and racemic molecules are shown. As the molecular structure is considered in more detail in all its spatially distributed features, the chirality is gradually manifested in its interaction. Thus, chiral interaction is stronger with more coarse-graining. Conversely, the chiral interaction gradually diminishes as one approximate the detailed anisotropic features of the molecular segments by sphericalization using equivalent spheres. In other words, chiral interaction is diminished with the gradual loss of chirality. The total molecular pair potential is gradually more dependent on the pairs of interactions, which are orientation dependent. These interaction centers are groups of molecules, as shown in Figures 5 and 6. One particular group of a molecule is oriented in an

asymmetric way with respect to the other groups of the neighboring molecule and the chirality is manifested by such spatial arrangements. In the equivalent sphere (ES) description, the chirality is considered at the lowest possible level with only four groups attached to a chiral center of a molecule (reduction of the spatial arrangement of groups to any further is not possible without losing the chirality). Thus, here the chirality of the molecule is suppressed in the pair potential. As a result, $\Delta U_{\min}/k_B T$ is small. However, distinctive homochiral preference is observed as shown in Table 2. It is interesting to note that, in the CG-5 model, the LJ parameters (diameters and energy parameters) of the constituent groups are scaled down by a factor of $1/5$, compared to the LJ parameters of the constituent groups of the ES model. However, the discriminating pair potential in CG-5 becomes 4.5 times more stable than in ES as shown in the fifth column of Table 2. However, despite the large variation in the parameters, the chiral preference remained unaltered and is significantly homochiral in all cases (from ES to CG-5). This is observed both in the packing as well as in the magnitude of the minimum of the pair potential (Table 2). We thus proceed to calculate the chiral discrimination energy for chiral amphiphiles on the basis of the ES approach.

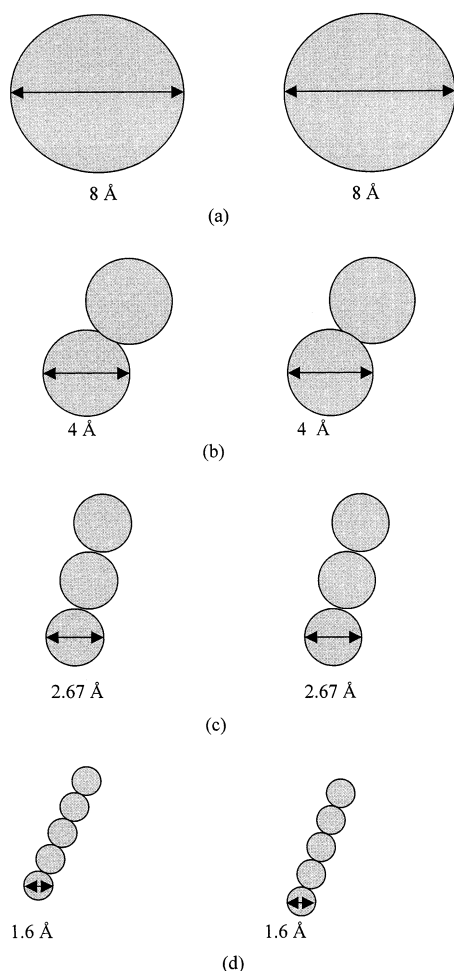


Figure 6. Gradual coarse-graining of two LJ equivalent spheres into smaller units (two, three, and five units).

TABLE 1: Parameters for the Calculation to Study the Effect of Coarse-Graining as Described in Section 2.A and Shown in Figures 5 and 6, Respectively^a

model	$\alpha(t)$	$\sigma(t)$	$\epsilon(t)/k_B$	$\mu(t)$	$\alpha(h)$	$\sigma(h)$	$\epsilon(h)/k_B$
ES	45.0	8.0	800.0	25.0	35.0	9.0	900.0
CG-2	45.0	4.0	400.0	25.0	35.0	4.5	450.0
CG-3	45.0	2.7	267.0	25.0	35.0	3.0	300.0
CG-5	45.0	1.6	160.0	25.0	35.0	1.8	180.0

^a Data are presented for enantiomeric pairs for which the parameters are the same for both molecules. In the case of a racemic pair, the first molecule has the orientations of the groups as the orientation of the mirror image of the groups of the second molecule. Temperature is 293.15 K in all cases.

The necessary parameters for the calculation and results of the ES-based calculation of the chiral discrimination of SSME, PAA, and TDHPAA are shown in Tables 3 and 4, respectively. In all cases, pairs of enantiomeric molecules are more compactly packed compared to the racemic pair. This is reflected in the Δr_{\min} , which is the difference of the separation of the chiral centers at the minimum of the pair potential of racemic and enantiomeric pairs. The closer packing of enantiomeric monolayers suggests homochiral preference. Homochiral preference is also seen in the behavior of $\Delta U_{\min}/k_B T$, which is negative in all cases. The homochiral preference can be observed in the domain shapes of the racemates of Figures 1–3. In Figure 1, the enantiomeric domains (either *R* or *S*) branch in a specific direction (Figure 1a and 1b, respectively). Similarly, in the case of *N*-stearoyl serine methyl ester monolayer, the enantiomeric domains (either *R* or *S*) are curved in a specific direction (Figure

TABLE 2: Results of the Calculation Using the Parameters of Table 1^a

model	chirality of pair	r_{\min}	$U_{\min}/k_B T$	$\Delta U_{\min}/k_B T$
ES	En	9.8	-5.22	-1.55
	Ra	15.2	-3.67	
CG-2	En	5.4	-5.77	-3.85
	Ra	12.8	-1.92	
CG-3	En	3.6	-6.56	-5.28
	Ra	12.0	-1.28	
CG-5	En	2.2	-7.78	-7.01
	Ra	11.4	-0.77	

^a “En” indicates enantiomeric pair, and “Ra” indicates racemic pair. r_{\min} is the separation of the chiral centers at the minimum pair potential, which is $U_{\min}/k_B T$. $\Delta U_{\min}/k_B T$ is the difference of the minimum pair potential of enantiomers and racemates ($[U_{\min}(\text{En}) - U_{\min}(\text{Ra})]/k_B T$). Mutual orientation is not allowed between molecules. Temperature is 293.15 K in all cases.

TABLE 3: Parameters Necessary for Calculation of the Discriminating Pair Potential of *N*-Stearoyl Serine Methyl Ester (SSME), *N*-Palmitoyl Aspartic Acid (PAA), and *N*-Tetradecyldihydropentanoic Acid Amide (TDHPAA)^a

molecule		σ (Å)	$\epsilon/k_B T$	μ (in deg)
SSME	t	8.72	1138.14	48
	h	3.55	355	
	a	2.71	271	
PAA	t	8.4	1068.33	31
	h	3.8	376	
	a	3.17	317	
TDHPAA	t	8.5	850	37.5
	h	2.71	271	
	a	2.96	296	

^a For details of the parameters and calculation see ref 9. Temperature is 297.15 K for SSME, 298.15 K for PAA, and 288.15 K for TDHPAA.

TABLE 4: Results of the Calculation Using the Parameters of Table 3

model	chirality of pair	r_{\min}	$U_{\min}/k_B T$	Δr_{\min}	$\Delta U_{\min}/k_B T$
SSME	En	15.4	-5.26	0.6	-0.80
	Ra	16.0	-4.46		
PAA	En	16.0	-5.01	0.4	-0.78
	Ra	16.4	-4.23		
TDHPAA	En	14.8	-4.62	2.5	-1.31
	Ra	17.3	-3.31		

^a “En” indicates enantiomeric pair, and “Ra” indicates racemic pair. r_{\min} is the separation of the chiral centers at the minimum pair potential, which is $U_{\min}/k_B T$. $\Delta U_{\min}/k_B T$ is the difference of the minimum pair potential of enantiomeric and racemic pairs ($[U_{\min}(\text{En}) - U_{\min}(\text{Ra})]/k_B T$). Δr_{\min} is the difference of the separation of the chiral centers at the minimum of pair potential of racemic and enantiomeric pairs. Temperature is 297.15 K for SSME and 298.15 K for PAA.

2a,b). The handedness of the enantiomeric domains is explained earlier.¹⁰ However, the racemic domains show the development of curvatures in both directions (Figure 2c,d, respectively). This is possible when the racemic domains composed of *R*- and *S*-molecules segregate in the domain and the curvature develops according to the handedness preferred by the enantiomer present in the segregated regions. Such chiral symmetry breaking is preferred by multiple factors, such as the closer packing of the enantiomers and the lower pair potential of enantiomeric pairs, compared to the racemic pairs.

We compare the discriminating features of the pair potentials of SSME, PAA and TDHPAA in Figures 7, 8, and 9, respectively. The pair potentials of enantiomers and racemates are different for different values of orientations of neighboring molecules. In all cases, the pair potential of the racemates are shallow compared to that of the enantiomers. We truncated the

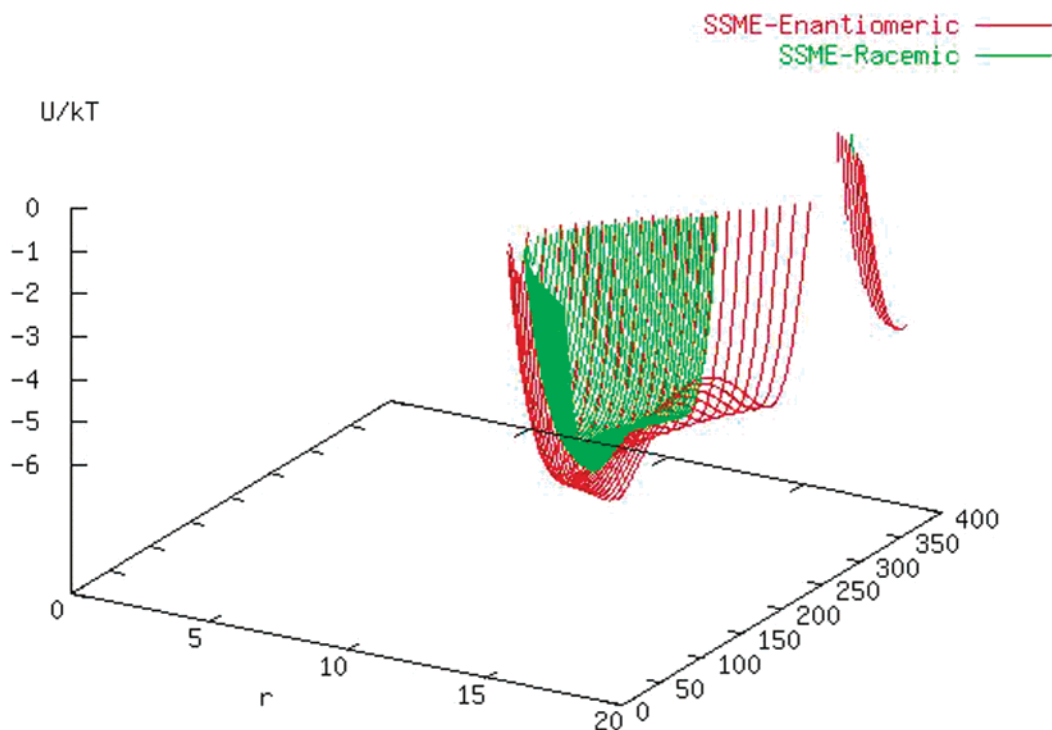


Figure 7. Comparison of the effective pair potentials of enantiomeric and racemic *N*-stearoyl serine methyl ester (SSME) molecules. The enantiomeric pair potential is marked as red, and the racemic pair potential is marked as green. The mutual orientation between the pair of molecules is expressed in degrees and varied from 0° to 360°. The intermolecular separation is expressed as r . Parameters necessary for the calculation are shown in Table 3. Temperature is 297.15° K.

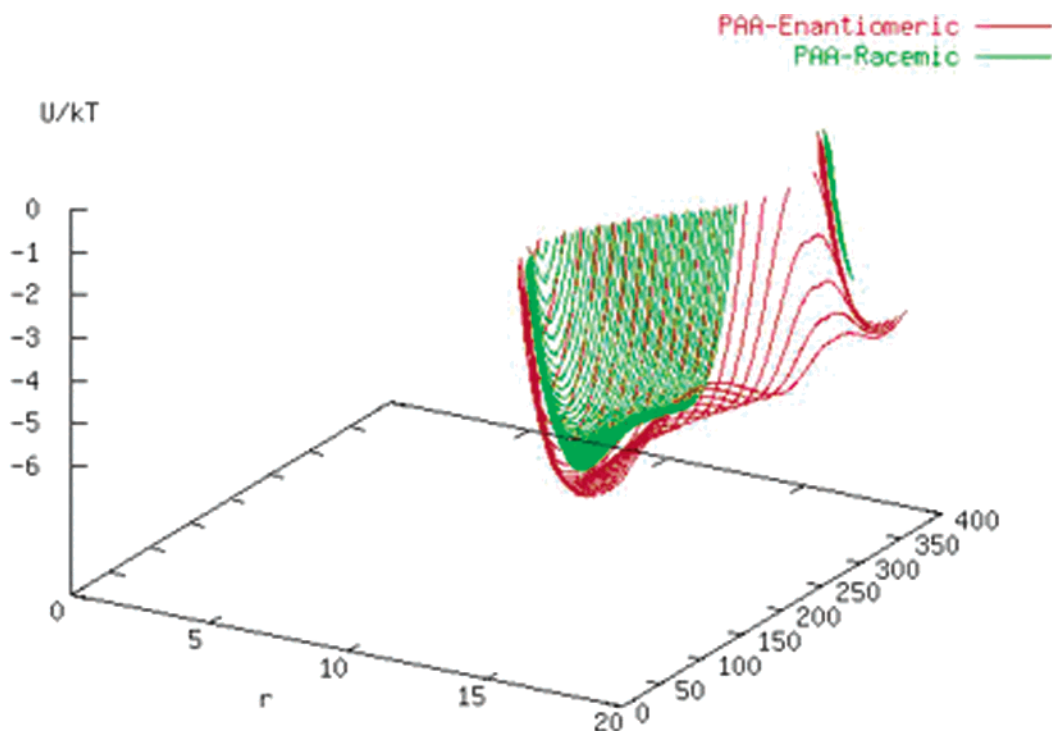


Figure 8. Comparison of the effective pair potentials of enantiomeric and racemic *N*-palmitoyl aspartic acid (PAA) molecules. The enantiomeric pair potential is marked as red, and the racemic pair potential is marked as green. The mutual orientation between the pair of molecules is expressed in degrees and varied from 0° to 360°. The intermolecular separation is expressed as r . Parameters necessary for calculation are shown in Table 3. Temperature is 298.15 K.

pair potential at 20 Å to make the minima clearly visible. However, the long-range part of the potential is also different for enantiomers and racemates (not shown in figures).

In the introduction we indicated that the ES-based effective pair potential model (model used in the present paper) and the tripodal model consider the molecular geometry in a different

way. In the present EPP-based theory, the orientations of the molecular segments are considered in detail (taken from experimental data), whereas the tripodal model neglects these orientations in the calculation of potential. The tripodal model further neglects any interaction related to the tail (tail–tail, tail–head as well as tail–side group attached to the chiral center).

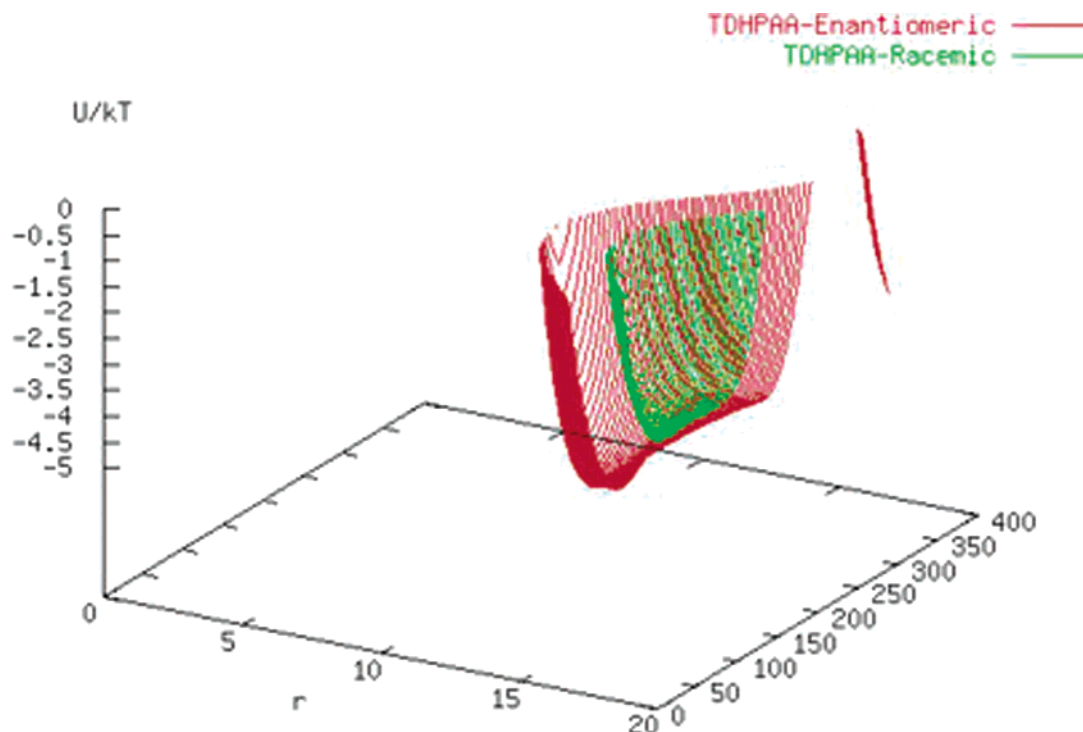


Figure 9. Comparison of the effective pair potentials of enantiomeric and racemic *N*-tetradecyldihydroxypentanoic acid amide (TDHPAA) molecules. The enantiomeric pair potential is marked as red, and the racemic pair potential is marked as green. The mutual orientation between pair of molecules is expressed in degrees and varied from 0° to 360° . The intermolecular separation is expressed as r . Parameters necessary for the calculation are shown in Table 3. Temperature is 288.15 K.

These orientation dependent interactions give nontrivial and nonnegligible contributions to the pair potential. It is thus instructive to compare the results of the two approaches.

In the tripodal model, heterochirality is found to be preferred when the LJ potential is used. When the tripodal model is applied to calculate the discrimination parameters for monolayers, heterochirality is again observed. Another interesting observation of the tripodal model is that the pair energy may change as a function of the inter-pair distance. Homochirality is observed to be preferred at shorter distances, whereas heterochirality is preferred at larger separations. From the present calculation, the magnitude of the *minimum* pair potential for all three chiral amphiphiles are observed as lower for the enantiomeric pair compared to the racemic pair. This is the signature of homochiral preference. However, in view of the complicated pair potential profile of the amphiphiles, the question arises whether the pair potential of the enantiomeric pair is always deeper than that of the racemic pair or may be the situation reversed for some values of distance and orientation. In the latter case, the pair potentials should exhibit heterochiral preference. To understand this, we calculated the difference in the pair potential of enantiomeric and racemic SSME. We consider a large range of intermolecular separation and orientational range from 0° to 360° . However, we select only the negative pair potentials because only the negative EPPs are relevant in determining the stable monolayer morphology. The difference in the pair potential is $\Delta U = (U(\text{enantiomeric}) - U(\text{racemic}))/k_B T$. The magnitude of ΔU for homochiral preference will be negative whereas for heterochiral preference the magnitude will be positive (the individual U values being negative for both the enantiomeric and racemic pairs).

The values of $(U(\text{enantiomeric}) - U(\text{racemic}))/k_B T$ are shown in Figure 10a for a large range of distance (the intermolecular separation is scaled by the distance at the minimum energy for the enantiomeric pair; the latter quantity is denoted by r_{\min}) and

orientation. The difference is found to be nonmonotonic. While significant homochirality is found at close packing separation (the intermolecular separation is of the order of r_{\min}), a small hump is observed for a certain range of orientation and distance, which is an indication of heterochirality (ΔU is positive). The chiral preference (either homo- or hetero-) vanishes at large separation where chiral interaction becomes insignificant, and we observe a flat plateau.

Homochiral preference is clearly shown at close separation (up to a separation of nearly 1.5 times of r_{\min}) in Figure 10b by significant negative values observed for ΔU . It is important to note that heterochirality is not observed within this range. The homochirality is also a non-monotonic function of the orientation. Explicitly, for a particular intermolecular separation, $(U(\text{enantiomeric}) - U(\text{racemic}))/k_B T$ varies with the orientation.

However, a significant heterochiral preference is observed for a certain range of distance (beyond a factor of 2 of r_{\min} and up to approximately a factor of 3 of it) and orientation (Figure 10c). The absolute magnitude of ΔU showing heterochirality is, however, much less than the absolute magnitude of ΔU showing homochirality.

Thus, the present calculation is in agreement with the conclusion of the tripodal model that the pair energy may change as a function of inter-pair distance. Homochirality is found to be preferred at shorter intermolecular separations, whereas heterochirality is preferred at larger separations according to tripodal model as well as the present EPP-based model. However, another significant and new observation of the present calculation is that the chiral discrimination is also a function of the orientation. This conclusion cannot be compared with the tripodal model because the latter neglects the orientation dependence of the intermolecular separation. The physical significance of the distance and orientation dependence of ΔU (observed from the present calculation) is that the enantiomeric molecules have a lower pair potential (more stability) at a large

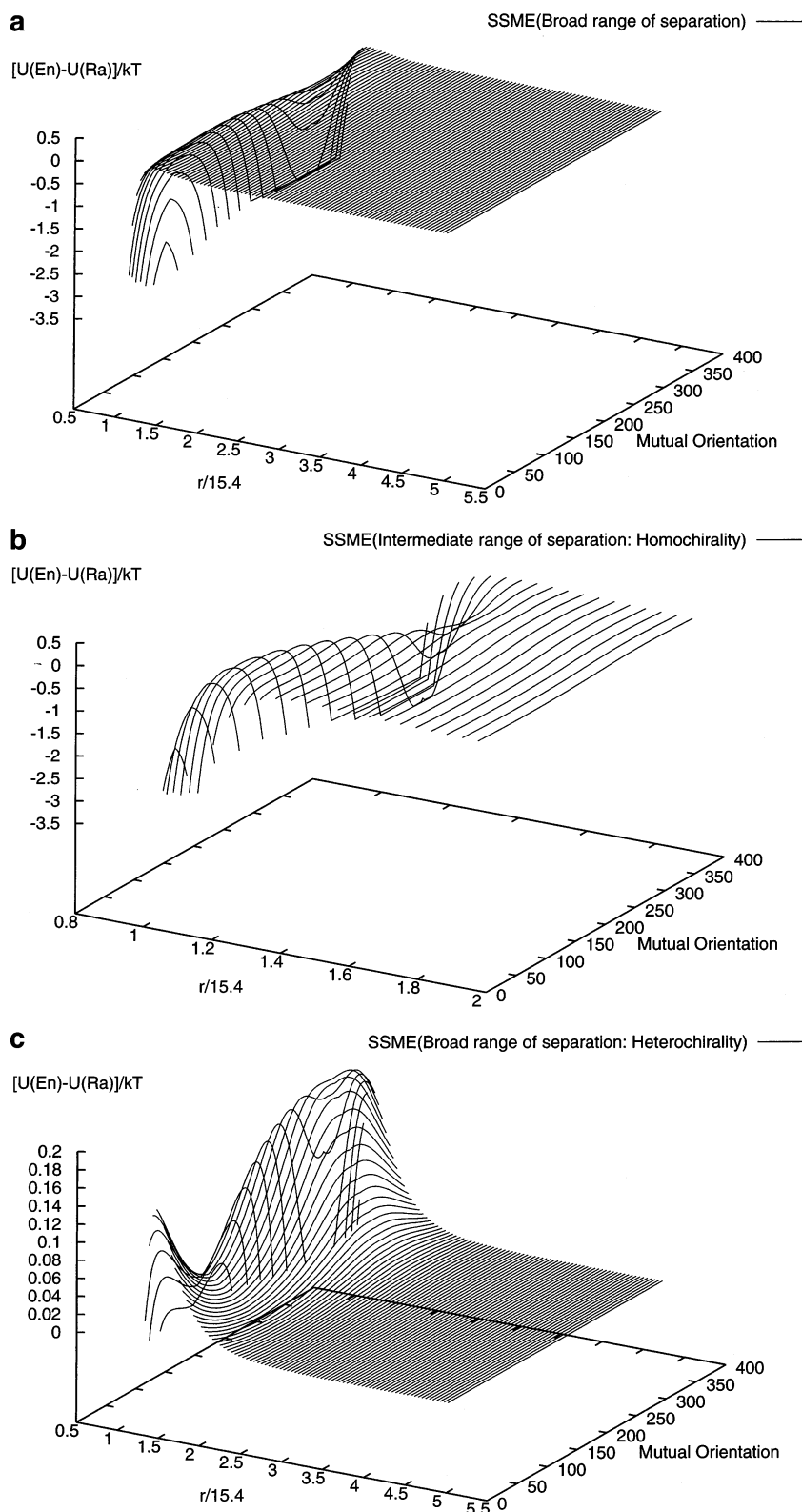


Figure 10. (a) The values of $(U(\text{enantiomeric}) - U(\text{racemic}))/k_B T$ for *N*-stearoyl serine methyl ester (SSME) molecule. The range of $(U(\text{enantiomeric}) - U(\text{racemic}))/k_B T$ is 0.5 to -3.5 . The mutual orientation between pair of molecules is expressed in degrees and varied from 0° to 360° . The variation in intermolecular separation is broad and varied from close separation to 61.6 \AA . The axis is expressed as $r/15.4$ (the minimum EPP is found in 15.4 \AA). Parameters necessary for the calculations are shown in Table 3. Temperature is 297.15 K . (b) The values of $(U(\text{enantiomeric}) - U(\text{racemic}))/k_B T$ for *N*-stearoyl serine methyl ester (SSME) molecule. The range of $(U(\text{enantiomeric}) - U(\text{racemic}))/k_B T$ is 0.5 to -3.5 . The mutual orientation between pair of molecules is expressed in degrees and varied from 0° to 360° . The variation in the intermolecular separation is intermediate and varied from close separation to 30.8 \AA . The axis is expressed as $r/15.4$ (the minimum EPP is found within 15.4 \AA). Parameters necessary for the calculations are shown in Table 3. Temperature is 297.15 K . (c). The values of $(U(\text{enantiomeric}) - U(\text{racemic}))/k_B T$ for *N*-stearoyl serine methyl ester (SSME) molecule. The range of $(U(\text{enantiomeric}) - U(\text{racemic}))/k_B T$ is $0-0.2$. The mutual orientation between the pair of molecules is expressed in degrees and varied from 0° to 360° . The variation in the intermolecular separation is very large and varied from close separation to 107.8 \AA . The axis is expressed as $r/15.4$ (the minimum EPP is found within 15.4 \AA). Parameters necessary for the calculations are shown in Table 3. Temperature is 297.15 K .

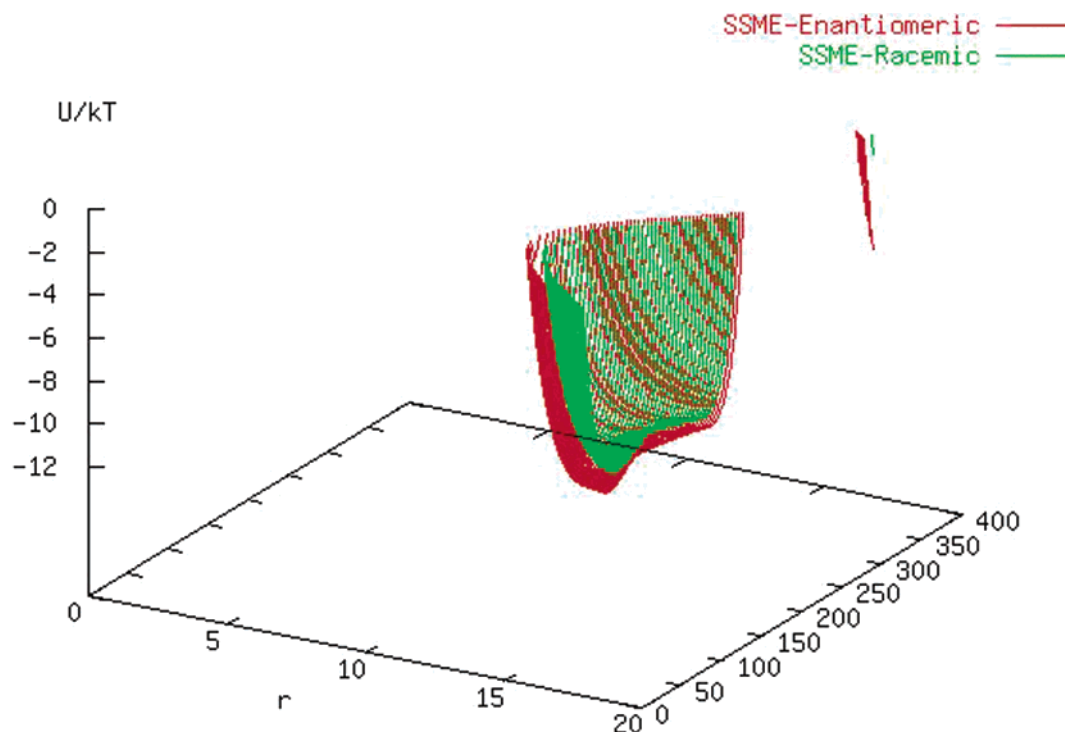


Figure 11. Comparison of the effective pair potentials of enantiomeric and racemic *N*-stearoyl serine methyl ester (SSME) molecules with variation in parameters. The enantiomeric pair potential is marked as red, and the racemic pair potential is marked as green. The mutual orientation between the pair of molecules is expressed in degrees and varied from 0° to 360° . The intermolecular separation is expressed as r . Energy parameters necessary for the calculation (ϵ/k_B) are doubled compared to those used in calculations corresponding to Figure 7. Temperature is 297.15 K.

range of orientations and smaller intermolecular separations compared to the pair potential of the racemic pairs when chiral molecules are compressed. At larger separations (more than a factor of 2 of r_{\min}) the pair potential of the racemic pairs become more stable than the enantiomeric pairs over a certain range of orientations. Beyond a large separation compared to r_{\min} the chiral interaction vanishes. However, it is possible that the molecular chiral structure as well as the parameters, such as azimuthal orientation and tilt angle, possibly play an important role in determining the chiral preference. More studies on different systems are necessary before generalizing the results.

It would be useful to compare the theoretical results obtained for chiral preference with further experimental information available at the molecular length scale, for example, as available from GIXD data. However, such data are needed for a substantial pressure range. A previous comparison between the CG and ES approach indicates that the coarse-grained molecular model is more suitable for a comparison with experimental results, because discrimination would be more apparent in the CG model. However, the calculations of the CG model are computationally extensive. Such a comparison could be the subject of further investigations.

It is necessary to comment the sensitivity of the result to the choice of parameters used in the calculations. The experimental parameters such as molecular tilt, azimuthal orientation or lattice angles are taken from GIXD data. The molecular structural and energy parameters are obtained either from the literature or by standard procedures. It is known that the effective diameters of the groups can be calculated with sufficient accuracy and represent the anisotropic shape of the long chain molecules quite well.^{22,23} These parameters can reproduce several liquid state properties fairly accurately.²³ However, the question arises how uncertainty in the (ϵ/k_B) parameters affect the results of chiral discrimination. Note that the depth of the pair potential well is determined by the corresponding set of the used ϵ/k_B parameters.

For a particular set of effective diameter and orientation, the variation of the ϵ/k_B parameter affects only the depth of the well, i.e., the minimum (for a smaller energy parameter, the well becomes shallow and vice versa). It is important that the pair potential is reasonably stable (negative) when compared to the $k_B T$ scale so that the mutual orientation observed at minimum (favored by the chiral interaction) is not destroyed by thermal motion. Now, if a single set of energy parameters of tail, head, and side chains is used in calculating the pair potential of the enantiomeric and racemic pair, the result about the discrimination is not affected by the choice of such parameters. The change in the value of the energy parameters from one set to the other will, of course, affect the depth of the well. However, the change will similarly affect both enantiomeric and racemic. As a result the conclusion about the discrimination will remain unaffected.

By varying the ϵ/k_B parameters in the SSME system for a large range, the above conclusion can be proved. We consider two cases to vary the parameters. In one case we double all ϵ/k_B parameters of the groups and in the other case we make all the parameters as half of those used in Table 3. The results show that the conclusion about homochirality remains unaffected by such a drastic change of the parameters. The plots are shown in Figure 11 (with a doubled energy parameter compared to the parameters used in Figure 7.) and Figure 12 (with half of the energy parameters used in Figure 7), respectively. It is clearly seen that whereas the individual pair potentials increase (when the energy parameters are doubled) or decrease (when the energy parameters are lowered), the discrimination between them remains unaltered, i.e., homochirally preferred. However, it is obvious that one should consistently use one chosen set to investigate the chiral interaction of both enantiomeric and racemic interaction and must not use different parameters (other than the experimentally observed parameters, such as azimuthal projection, tilt, etc.). It is important to note that Andelman and

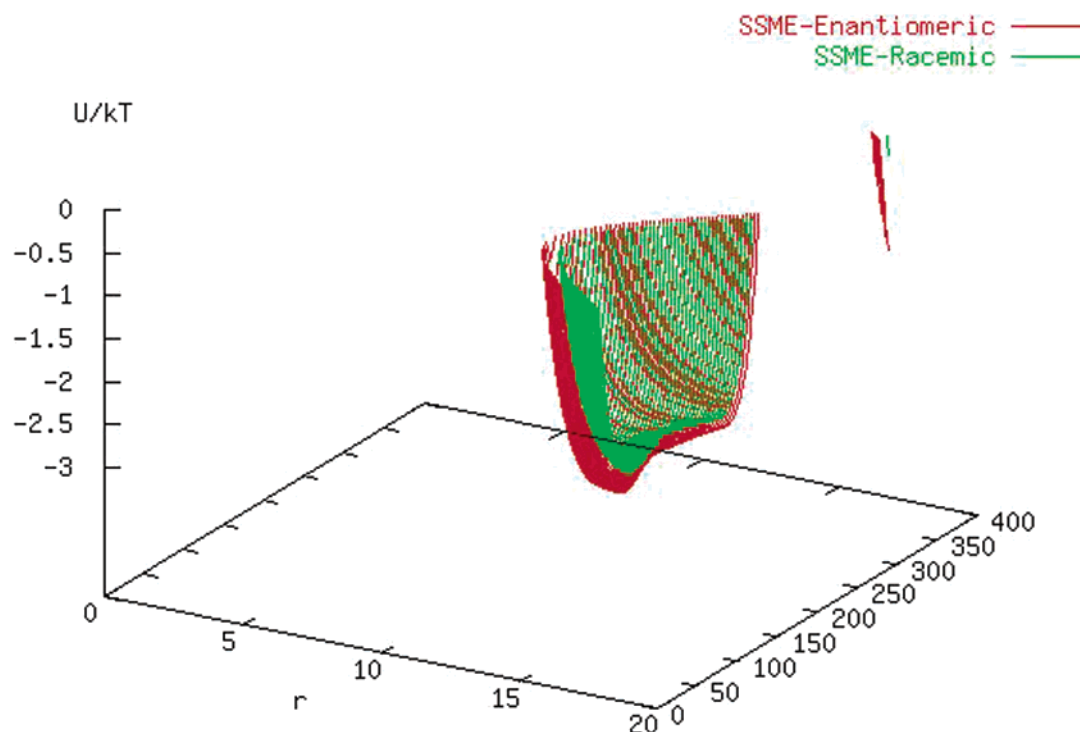


Figure 12. Comparison of the effective pair potentials of enantiomeric and racemic *N*-stearoyl serine methyl ester (SSME) molecules with variation in parameters. The enantiomeric pair potential is marked as red, and the racemic pair potential is marked as green. The mutual orientation between the pair of molecules is expressed in degrees and varied from 0° to 360° . The intermolecular separation is expressed as r . Energy parameters necessary for the calculation (ϵ/k_B) are half-compared to those used in calculations corresponding to Figure 7. Temperature is 297.15 K.

Orland also used representative parameter values of diameter and energy for the model tetrahedral molecule.⁴

Conclusions

In conclusion, we carried out theoretical studies about the chiral discrimination energies in the condensed phase domains of chiral amphiphilic monolayers. Studies on model systems show that the depth of the potential is well-dependent on the coarse-graining and may not be the same for the detailed coarse-grained and equivalent-sphere-based approach. However, systematic coarse-graining of the molecule shows that the use of a consistent set of parameters does not affect the conclusion about the chiral preference (homo- or heterochirality) although the exact magnitudes of the pair potentials are dependent on the extent of coarse-graining. This indicates that with a gradual loss of chirality of the molecule, the chiral interaction is diminished. This conclusion fairly corroborates the common knowledge. Calculations of the chiral discriminating pair potential of three different amphiphiles indicate homochiral preference. The preference is observed both in the packing and pair potential energy. The homochiral preference corroborates well the observed domain features of the racemates where growths in opposite directions are observed. The growth in both directions is indicative of local chiral symmetry breaking which is possible in the homochirally preferred interaction. We also compare the results of calculation of discrimination energy by present approach and the results by other molecular models (tripodal model) available in the literature. Whereas the basic conclusions of the present approach and the tripodal model agree, the present model reveals nontrivial distance and orienta-

tion dependence of the discrimination energy. The results of the calculation are shown to be tolerant of large parameter variations.

References and Notes

- (1) McConnell, H. M.; Moy, V. T. *J. Phys. Chem.* **1988**, *92*, 4520.
- (2) Andelman, D.; de Gennes, P.-G. *C. R. Acad. Sci., Ser. II (Paris)* **1988**, *307*, 233.
- (3) Andelman, D. *J. Am. Chem. Soc.* **1989**, *111*, 6536.
- (4) Andelman, D.; Orland, H. *J. Am. Chem. Soc.* **1993**, *115*, 12322.
- (5) Melzer, V.; Weidemann, G.; Vollhardt, D.; Brezesinski; Wagner, R.; Struth, B.; Möhwald, H. *J. Phys. Chem. B* **1997**, *101*, 4752.
- (6) Nandi, N.; Bagchi, B. *J. Am. Chem. Soc.* **1996**, *118*, 11208.
- (7) Nandi, N.; Bagchi, B. *J. Phys. Chem.* **1997**, *101*, 1343.
- (8) Krüger, P.; Lösche, M. *Phys. Rev. E* **2000**, *62*, 7031.
- (9) Nandi, N.; Vollhardt, D. *Colloids Surf. A* **2001**, *183*, 67.
- (10) Nandi, N.; Vollhardt, D. *Colloids Surf. A* **2002**, *198*, 207.
- (11) Nandi, N.; Vollhardt, D. *J. Phys. Chem.* In press.
- (12) Weis, R. M.; McConnell, H. M. *Nature* **1984**, *310*, 47.
- (13) McConnell, H. M. *Annu. Rev. Phys. Chem.* **1991**, *42*, 171.
- (14) Möhwald, H. *Annu. Rev. Phys. Chem.* **1990**, *41*, 441.
- (15) Kaganer, V. M. et al. *Rev. Mod. Phys.* **1999**, *71*, 779.
- (16) Vollhardt D. et al. In *Short and Long Tails at Interfaces*, Proceedings of the 30th Rencontres De Moriond; Eds. Daillant, J., Guenoun, P., Marques, C., Muller, P., Trän, T. V. J., Eds.; Editions Frontiers: Cedex, France 1995; p 149.
- (17) Vollhardt, D. in *Encyclopedia of Surface and Colloid Science*; Hubbard, A., Ed.; Marcel Dekker, New York, 2002; p 3585.
- (18) Flapan, E. *When Topology Meets Chemistry: A Topological Look at Molecular Chirality*; Cambridge University Press: Cambridge, 2000.
- (19) Mason, S. F. *Chemical Evolution*; Clarendon Press: Oxford, U.K., 1991; Chapter 14.
- (20) Stinson, S. C. *Chem. Eng. News* **2001**, *79*, 45.
- (21) de Gennes, P. G.; Prost, J. *The Physics of Liquid Crystals*; Clarendon: Oxford, 1993.
- (22) Bondi, A. *J. Phys. Chem.* **1964**, *68*, 441.
- (23) Ben Amotz, D.; Herschbach, D. R. *J. Phys. Chem.* **1990**, *94*, 1038.